Robust Power System State & Topology Coestimation Based on Novel Information Theory Concepts

Rogerio Meneghetti Antonio Simões Costa
Federal University of Santa Catarina
Florianópolis, SC, Brazil
Emails: rogerio.meneghetti@posgrad.ufsc.br, simoes.costa@ufsc.br

Vladimiro Miranda
INESC TEC and University of Porto
Porto, Portugal
Email: vmiranda@inesctec.pt

***Abstract*—A recently proposed approach for power system state estimation based on novel Information Theory concepts is extended to allow the identification and automatic rejection of topology errors, in addition to bad data on analog measurements. The final result is a robust, self-healing state & topology coestimation method capable of providing reliable estimates even in the presence of both types of modeling errors. A two-level estimation architecture is assumed in which a conventional estimator based on the bus-branch network model is employed at the first level. Whenever modeling errors are detected and then properly localized, the second estimation level is activated. At that stage, the affected substations are modeled at bus-section level and the proposed state & topology coestimation approach is applied. Several case studies conducted with the IEEE 24-bus and 30-bus test systems are employed to assess the performance of the proposed methodology.**

Keywords — Multi-Level State Estimation, Topology Error Identification, Dad Data Processing, Power System Real-Time Modeling.

I. Introduction

Secure operation of electric power systems relies on the availability of reliable information about the system current operating conditions. Power System State Estimation (PSSE) is the EMS function responsible for building and continuously updating the real-time model of the electric network, and is thus a prime function for power system situational awareness. To perform its task, PSSE processes two types of data: (i) measurements of analog quantities collected by SCADA and possibly phasor monitoring systems, and (ii) network topology information. The latter is determined by the Network Configurator, another application which processes only digital data reflecting the statuses of circuit breakers and switches.

Among all possible factors that may affect PSSE performance, the occurrence of gross errors as part of its input data is probably the one that raises most concerns. This fact is connected with the well-known sensitivity of the Weighted Least-Squares PSSE solution to bad data. Procedures for detecting and identifying modeling errors were already outlined in Schweppe's seminal PSSE papers (see, for instance, [1]). Many research efforts have been devoted throughout the last decades to the development of methods for analog bad data processing, most of which are described in [2], [3]. Topology error identification has also been a topic of considerable interest due to the great impact of topology errors on state estimation results. Unlike analog bad data processing methods, which are usually conducted at bus-branch level, generalized PSSE methods that rely on modeling the power network at bus section level [2] are generally recognized as the most effective for topology error identification [4], [5]. By exploiting such a detailed modeling strategy as applied to suspect, limited-size subnetworks, some authors have proposed new forms of EMS applications to either perform topology estimation [6] or state and topology coestimation [7], [8].

Despite the above modeling and algorithmic advances, however, virtually all conventional bad data processing methods based on the WLS approach have as a common trait the need of re-estimating the states (and possibly the topology also) after the identified analog or digital gross errors have been properly identified and eliminated. This is so because the state & topology estimates obtained in the presence of such errors are irremediably compromised by their effects. The ensuing measurement set and network model adjustments require extra CPU time, what negatively impacts the efficiency of the whole real-time modeling process.

Lately, a new class of state estimation algorithms based on recently developments in Information Theory have been proposed to overcome the above difficulties. Accordingly, concepts such as maximum correntropy [9] and dynamically adjusted Parzen windows [10] have paved the way for this new generation of PSSE algorithms that exhibit remarkable self-healing properties in the presence of bad data. Since the Maximum Correntropy Criterion (MCC) leads to a non-quadratic objective function, the controlled adjustment of the Parzen windows along the iterations is important to properly steer the solution in order to avoid multiple solution traps that may occur in connection with non-quadratic optimization criteria. Reported research efforts based on the application of such concepts to PSSE [11]–[14] confirm the method's capability for automatically rejecting gross analog measurements while still providing good state estimates, without the need of extra runs of the state estimator.

This paper is aimed at extending the applicability of that novel PSSE approach based on Information Theory concepts in order to also enable the rejection of topology error effects, in addition to bad data on analog measurements. The expected result is a robust estimator capable of providing reliable state & topology estimates even in the presence of both types of modeling errors.

In order to pursue that objective, the Generalized State Estimation paradigm [15] is assumed, according to which PSSE is not a single, centralized procedure. Instead, it is conducted in two stages: the first one is performed by a conventional estimator based on the familiar bus-branch model, whereas the second stage is invoked whenever modeling errors are detected in the first stage. After bad data localization, a reduced subnetwork containing the suspect substations is identified as a "bad data pocket", which is then modeled at the bus-section level. Therefore, in the second estimation stage the circuit breakers pertaining to the reduced subnetwork are explicitly represented.

The algorithm applied in the second stage relies on the maximum Correntropy criterion combined with dynamically adjusted Parzen windows [11], [12], [14] . However, it must be adapted to comply with modeling at the bus-section level, as detailed in the remaining sections of this paper. A background review of the pertinent Information Theory concepts is also provided. In addition, results of case studies conducted with two distinct IEEE test systems are presented to illustrate the applicability of the proposed methodology.

II. PSSE Background

A. Bus-branch measurement model and Weighted Least-Squares Solution

The conventional approach for PSSE relies on the familiar bus-branch model for the electric network, in which the state vector $\boldsymbol{x}$ is formed by bus voltage phase angles and magnitudes. The state estimator processes SCADA measurements of bus voltage magnitudes, active/reactive branch power flows, and active/reactive bus power injections. The measurement model that relates measurements and state variables is given by:

$$\boldsymbol{z_m} = \boldsymbol{h_m}(\boldsymbol{x}) + \boldsymbol{\eta_m} \tag{1}$$

where the $m \times 1$ vectors $\boldsymbol{z_m}$, $\boldsymbol{h_m}(\boldsymbol{x})$ and $\boldsymbol{\eta_m}$ are the measurement vector, the vector of nonlinear functions relating measured quantities and state variables, and the vector of random measurement errors, respectively. The latter is assumed to be uncorrelated, normally distributed, with zero mean and covariance matrix $\boldsymbol{R_m}$, that is

$$\boldsymbol{E\{\eta_m\} = 0} \;\; ; \;\; \boldsymbol{E\{\eta_m \eta_m^T\} = R_m} \tag{2}$$

Due to above uncorrelatedness assumption, $\boldsymbol{R_m}$ is diagonal.

State estimation is usually formulated as a Weighted Least Squares (WLS) problem whose objective function to be minimized is

$$J(\hat{\boldsymbol{x}}) = [\boldsymbol{z_m} - \boldsymbol{h_m}(\hat{\boldsymbol{x}})]^{\boldsymbol{T}} \boldsymbol{R_m^{-1}} [\boldsymbol{z_m} - \boldsymbol{h_m}(\hat{\boldsymbol{x}})] \tag{3}$$

The minimization of (3) leads to an iterative process in which the well known Gauss normal equation [2], [3] is solved in each iteration in order to provide new state iterates $\hat{\boldsymbol{x}}$ until convergence is reached. Bad data detection and identification procedures [2], [3] are then performed in order to determine if modeling errors such as bad data on analog data or incorrect network topology are present and contaminate the PSSE solution.

B. Network modeled at bus-section level

In generalized state estimation [15], the above outlined WLS procedure constitutes the first PSSE stage. In case the associated bad data processing routines indicate the presence of modeling errors, bad data localization is exploited in order to determine a suspect region of the network containing such errors. The second estimation stage then starts by modeling the substations within such subnetwork at the bus-section level, and circuit breakers pertaining to those substations are explicitly represented. To accomplish that, active and reactive power flows through those switching branches are defined as new state variables, in addition to the nodal voltage states [6], [16]. Therefore, if n_{sb} denotes the number of switching branches, the size of the augmented state vector is $n = 2N + 2n_{sb} - 1$, where N is the number of network buses.

Switching branch modeling relies on the relationships between their state variables, and depends on the corresponding status [2]. They define the so-called *operational conditions*, as follows. If switching branch $i - j$ is assumed closed, the voltage drop across its terminals must be null, that is:

$$\delta_i - \delta_j = 0 \;\; ; \;\; V_i - V_j = 0. \tag{4}$$

On the other hand, an open switching branch is characterized by zero power flows through it:

$$p_{ij} = 0 \;\; ; \;\; q_{ij} = 0. \tag{5}$$

The set of N_o operational conditions (4) and (5) for all modeled switching branches are collectively represented by

$$\boldsymbol{h_o}(\boldsymbol{x}) = \boldsymbol{0}. \tag{6}$$

In addition to the operational conditions, the model at bus-section level must also include the KCL equations for the new electrical nodes that arise as a result of the interconnection within substations involving bus sections, circuit breakers and conventional branches (i.e, lines and transformers) [2]. They compose a set of N_s mathematical relationships and are referred as *structural conditions*:

$$\boldsymbol{h_s}(\boldsymbol{x}) = \boldsymbol{0}. \tag{7}$$

C. A Priori State Information

When dealing with a sequence of evolving network topologies, aggregating *a priori* state information (APSI) to PSSE is a convenient means to circumvent possible observability problems which otherwise would prevent reaching a solution. This is a much more attractive artifice than the alternative of dynamically defining multiple angle references for each connected component of the electrical network graph. As a subproduct, APSI also helps to preserve the numerical stability of the estimation problem [17].

Defining $\bar{\boldsymbol{x}}$ as the vector of *a priori* information on the state variables and $\boldsymbol{\Sigma}$ is the corresponding covariance matrix, APSI can be included in the PSSE problem by augmenting the objective function (3) with the term

$$\frac{\mathbf{1}}{\mathbf{2}}(\hat{\boldsymbol{x}} - \bar{\boldsymbol{x}})^{\boldsymbol{T}}\boldsymbol{\Sigma}^{\mathbf{-1}}(\hat{\boldsymbol{x}} - \bar{\boldsymbol{x}}) \tag{8}$$

Matrix $\boldsymbol{\Sigma}$ is usually assumed diagonal, and its diagonal entries reflect the degree of confidence on the *a priori* state information. In practice, only nodal voltage states matter, so that only the corresponding $\boldsymbol{\Sigma}^{\mathbf{-1}}$ entries are nonzero, with values that are some degrees of magnitude less than the those in $\boldsymbol{R}_{\boldsymbol{m}}^{\mathbf{-1}}$. This ensures that under observable conditions APSI will have little influence on the state estimates.

III. Maximum Correntropy Criterion and Parzen Windows

Unlike conventional PSSE methods, which minimize a weighted least-squares objective function, the Maximum Correntropy Criterion is aimed at maximizing the information extracted from the available set of measurements [11]–[14]. The Correntropy concept can be interpreted as a measure of similarity between measured and estimated values within a given observation window. The latter is defined by using the Parzen window concept [10], which is essentially a Gaussian kernel κ_σ centered on each state iterate $\hat{\boldsymbol{x}}^{\boldsymbol{k}}$ and whose width σ can be controlled. For a given measurement i, this kernel function is given by

$$\kappa_\sigma(z_i - h_i(x^k)) = \frac{1}{\sqrt{2\pi}\sigma_i} e^{-\frac{(z_i - h_i(x^k))^2}{2\sigma_i^2}} \tag{9}$$

From (9), the Correntropy function $\mathcal{V}$ considering the whole set of measurements is then defined as

$$\mathcal{V}(\boldsymbol{z}, \boldsymbol{h}(\boldsymbol{x}^{\boldsymbol{k}})) = \frac{1}{m}\sum_{i=1}^{m} \kappa_\sigma(z_i - h_i(x^k)) \tag{10}$$

Neglecting the constant factors in (9) and (10) that have no effect on optimization, the objective function to be maximized according to the MCC approach is

$$J_{MCC} = \sum_{i=1}^{m} e^{-\frac{(z_i - h_i(x^k))^2}{2\sigma_i^2}} \tag{11}$$

The window width parameter σ has an important role in the iterative optimization process. For large σ values, the MCC solution practically coincides with the WLS one, since in that case Correntropy reduces itself to the Euclidean norm of the residuals [11], [12]. Under such conditions, it is well known that the final estimates are much affected by the presence of outliers within the measurement set. On the other hand, by adopting a proper strategy for dynamically adjusting σ along the iterative process, weights assigned to measurements with large residuals are progressively reduced, so that outliers are eventually rejected. This is tantamount to applying other less sensitive norms such as L_1 or even L_0 to those measurements, what substantially decreases their influence on the final estimates.

IV. State and Topology Coestimation based on the Maximum Correntropy Criterion

A. MCC Inner Loop

As described in Section II-B, state estimation performed at the second estimation level relies on a detailed bus-section network model. Therefore, both the operational and structural conditions of equations (6) and (7) must be taken into account in the problem formulation, together with measurement equation (1). For that purpose, we follow the procedure originally proposed in [18], according to which *both operational and structural conditions are treated as pseudo-measurements*. As a result, the corresponding nonlinear functions are aggregated into a single observation vector, that is, $\boldsymbol{h}(\hat{\boldsymbol{x}}) = [\boldsymbol{h_m}(\hat{\boldsymbol{x}})^{\boldsymbol{T}}, \boldsymbol{h_s}(\hat{\boldsymbol{x}})^{\boldsymbol{T}}, \boldsymbol{h_o}(\hat{\boldsymbol{x}})^{\boldsymbol{T}}]^{\boldsymbol{T}}$. Likewise, we define $\boldsymbol{z} = [\boldsymbol{z}_{\boldsymbol{m}}^{\boldsymbol{T}}, \mathbf{0}^{\boldsymbol{T}}, \mathbf{0}^{\boldsymbol{T}}]^{\boldsymbol{T}}$ and $\boldsymbol{R} = diag\{\boldsymbol{R_m}, \boldsymbol{R_s}, \boldsymbol{R_o}\}$, where $\boldsymbol{R_s}$ and $\boldsymbol{R_o}$ are diagonal matrices that play the role of "covariance matrices" for the structural and operational conditions. In practice, the diagonal entries in $\boldsymbol{R_s}$ are small positive values ϵ_s, since the uncertainty related to the structural conditions is virtually null. On the other hand, relatively large positive values ζ_o are assigned to the $\boldsymbol{R_o}$ entries, to reflect the fact that circuit breaker statuses are assumed in this work as uncertain and subject to validation by the estimation process. The adopted values for ϵ_s and ζ_o are further discussed in Section V.

From the above definitions, the MCC objective function for state & topology coestimation considering also *a priori* information is defined as

$$J_{MCC_{S\&T}} = \sum_{i=1}^{M}\left[R_{ii}^{-1}.e^{-\frac{(z_i - h_i(\hat{x}))^2}{2\sigma_i^2}}\right] - \frac{1}{2}(\hat{\boldsymbol{x}} - \bar{\boldsymbol{x}})^T\boldsymbol{\Sigma}^{\mathbf{-1}}(\hat{\boldsymbol{x}} - \bar{\boldsymbol{x}}) \tag{12}$$

where $M = m + N_s + N_o$, and the negative sign before the second term on the right-hand side is due to the fact that Problem (12) is a maximization problem.

The application of the optimality conditions to Problem (12), after some algebraic manipulations, lead to the following linear system to be solved in each iteration:

$$\left[\boldsymbol{H}^{\boldsymbol{T}}\boldsymbol{W}\boldsymbol{H} + \boldsymbol{\Sigma}^{\mathbf{-1}}\right]\boldsymbol{\Delta x} = \boldsymbol{H}^{\boldsymbol{T}}\boldsymbol{W}\cdot\boldsymbol{\Delta\tilde{z}} + \boldsymbol{\Sigma}^{\mathbf{-1}}(\bar{\boldsymbol{x}} - \hat{\boldsymbol{x}}) \tag{13}$$

where

$$\boldsymbol{W} = \boldsymbol{D}[\boldsymbol{I} - \boldsymbol{R_p}] \ , \qquad R_{p,ii} = (z_i - h_i(\hat{x}^k))^2 \ / \sigma_i^2 \ ;$$
$$\boldsymbol{\Delta \tilde{z}} = [\boldsymbol{I} - \boldsymbol{R_P}]^{-1} \boldsymbol{\Delta z} \ , \quad D_{ii} = \frac{R_{ii}^{-1}}{\sigma_i^2} e^{-(z_i - h_i(\hat{x}^k))^2 \ / 2\sigma_i^2}. \tag{14}$$

In the above, $\boldsymbol{H}$ is the Jacobian matrix of $\boldsymbol{h(\cdot)}$ computed at point $\boldsymbol{\hat{x}^k}$, $\boldsymbol{\Delta z} = \boldsymbol{z} - \boldsymbol{h(\hat{x}^k)}$, and $\boldsymbol{I}$ is the $M \times M$ identity matrix. It should be emphasized that matrix $\boldsymbol{W}$ must be updated in each iteration, since it depends on the Parzen window width σ. After solving (13), the state variables are updated according to

$$\boldsymbol{\hat{x}^{(k+1)}} = \boldsymbol{\hat{x}^k} + \boldsymbol{\Delta x} \tag{15}$$

until $||\boldsymbol{\Delta x}||$ becomes less than a pre-specified tolerance. Iteratively solving equation (13) constitutes what we refer to as *iterative inner loop*. As discussed in the sequel, the strategy for adjusting parameter σ is implemented in the *iterative outer loop* of the MCC algorithm.

B. MCC Outer Loop

As discussed in Section III, the importance of parameters σ_i for granting the MCC bad data rejection properties is paramount. In this subsection, the iterative strategy for adjusting σ_i is described. For convenience, the term "measurement" is indistinctly applied to all input data to the estimator, regardless of being measurement or operational condition pseudo-measurement.

In a typical outer loop iteration, the estimation residuals $z_i - h_i(x^k), i = 1, ..., M$, are computed and compared with the current value of the corresponding σ_i. If the residual is larger than σ_i, then: *a*) measurement i is added to a set S of outliers, and *b*) its corresponding parameter σ_i is set at a small positive value, what amounts in practice to eliminating measurement i from state estimation (see (12)).

For the measurements that do not belong to set S, the Parzen window widths are updated according to

$$\sigma_i^{k+1} = \max_j |z_j - h_j(\hat{x}^k)| \quad i, j \in \{1, ..., M\} \setminus \{S\} \tag{16}$$

At the beginning of the outer loop, σ_i is set at a sufficiently large value for all input data, so that no available measurement is initially discarded. As the iterations evolve, the outliers are progressively withdrawn from the estimation process and stored in set S. Simultaneously, the updating mechanism in (16) gradually reduces the window width for the sound measurements, until a predetermined σ_{min} value is reached. Adjusting σ_{min} implies a trade off, since very small values may lead to identifying sound measurements as outliers, whereas too large values may preclude the identification of bad data. This issue is revisited in Section V.

C. Determining the Estimated Topology

Upon completion of the outer loop iterations outlined in the previous subsection, a set S of outliers is produced that may contain gross analog measurements and/or inconsistent operational pseudo-measurements related to switching branch statuses. In the latter case, it is still necessary to translate the errors flagged by the MCC estimator into topology information. This is accomplished through a hypothesis testing procedure applied to the estimated switching branch power flows [16]. From a pre-specified false alarm probability α, a threshold for those flows can be calculated in order to determine if a switching branch is open or closed. For a given switching branch ℓ, this threshold is given by (17)

$$\epsilon_{flow_\ell} = \sqrt{\Omega_{\ell\ell}}.N_{1-\frac{\alpha}{2}} \tag{17}$$

where $\Omega = (H^T R H)^{-1}$, and $N_{1-\frac{\alpha}{2}}$ is the $100(1 - \frac{\alpha}{2})$ percentile of the normal distribution.

V. Simulation results

A. Measurement simulation, parameters and performance indices

IEEE 24-bus and 30-bus test systems are employed to evaluate the performance of the MCC-based state & topology estimator. One line diagrams and bus-branch data for those networks can be found in [19]–[21]. All simulations have been conducted in Matlab using nonlinear network models. SCADA measurements of bus voltage magnitudes (denoted by V_i), active/reactive power injections (P_i/Q_i) and active/reactive power flows (t_{ij}/u_{ij}) are simulated by superposing randomly generated errors to values obtained from converged power flow cases. Assumed meter accuracies are equal to $0.01 \ pu$ for all types of measurements. Parameter ϵ_s used to specify matrix R_s is set to 1×10^{-6}, while parameter ζ_o connected with matrix R_o is set to three orders of magnitude greater than the average of the measurement variances, according to the rationale discussed in Section IV-A.

Two distinct metrics [22] are used to assess the quality of the state estimates provided by the MCC estimator, as follows:

$$M_V = \left(\frac{1}{N} \sum_{i=1}^{N} \left| \vec{V}_i^{estim} - \vec{V}_i^{true} \right|^2 \right)^{\frac{1}{2}} \tag{18}$$

$$M_S = \left(\frac{1}{n_{sb}} \sum_{i=1}^{n_{sb}} \left| \vec{S}_i^{estim} - \vec{S}_i^{true} \right|^2 \right)^{\frac{1}{2}} \tag{19}$$

In the above definitions, $\vec{V}$ and $\vec{S}$ stand for complex voltages at all network buses and complex power flows through the switching branches, respectively. In addition, superscripts *estim* and *true* stand for estimated and true (that is, obtained from the underlying power flow case) values.

An MCC-based state & topology estimation run is considered successful when: *a*) $M_V \leq 1\%$; *b*) $M_S \leq 2\%$, and *c*) the estimated topology is found to be the right one.

B. Results for the IEEE 24-bus system

The 24-bus test system and the corresponding metering scheme are shown in Fig. 1. The metering scheme is composed by the following measurements: 15 bus voltage magnitudes, 23 active/reactive power injection pairs, and 39 active/reactive power flow pairs (noticed that those numbers include also

measurements taken at the bus-section level, shown in Fig. 2). The substations that correspond in Fig. 1 to buses 14 and 16 have been selected as the ones where topology and/or analog measurement errors occur. Their models at the bus section level are presented in Fig. 2, where the switching branches are shown with their true statuses. The number of state variables for the test system when the two substations are represented at physical level raises to 93.

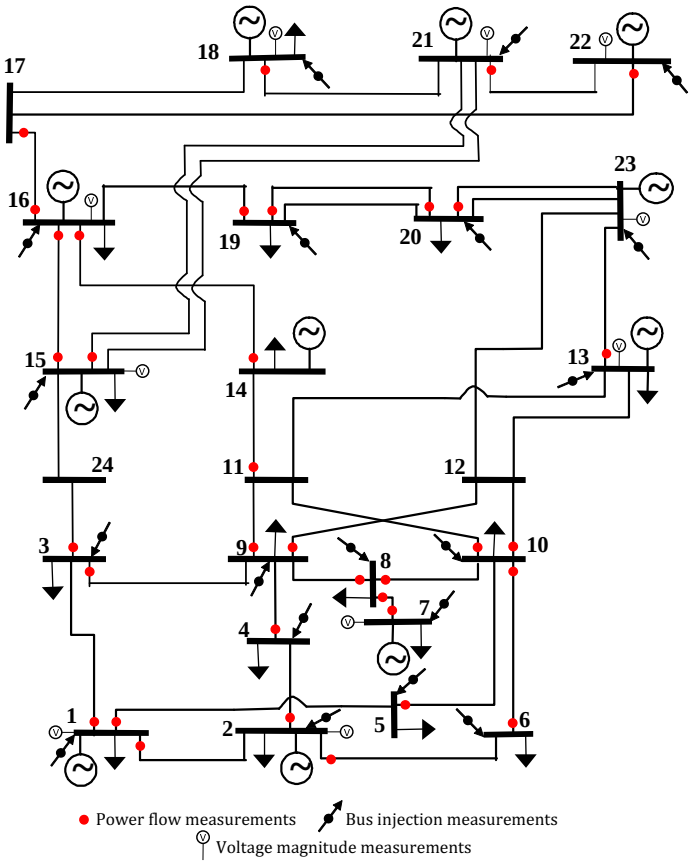

Fig. 1. IEEE 24-bus network.

Two case studies are conducted to illustrate the performance of the MCC-based state & topology coestimation approach: the first one considers that only the presumed topology is erroneous, whereas the second case also involves analog bad data.

1) Topology errors only: Branch 27-28 is erroneously excluded from the network model due to wrongly reported statuses of circuit breakers $B2$ and $B9$. Therefore, the presumed topology delivered to the state estimator is incorrect. It is assumed that bad data localization performed in connection with the first PSSE stage (see Section II) properly determines that the modeling errors are confined to substations 14 and 16.

Next, the second level state & topology coestimator is applied to the network with the two substations modeled at physical level. Parameter σ is initialized as 10 pu, and the updating algorithm described in Section IV-B is activated. Table I describes how σ values evolve along the outer loop

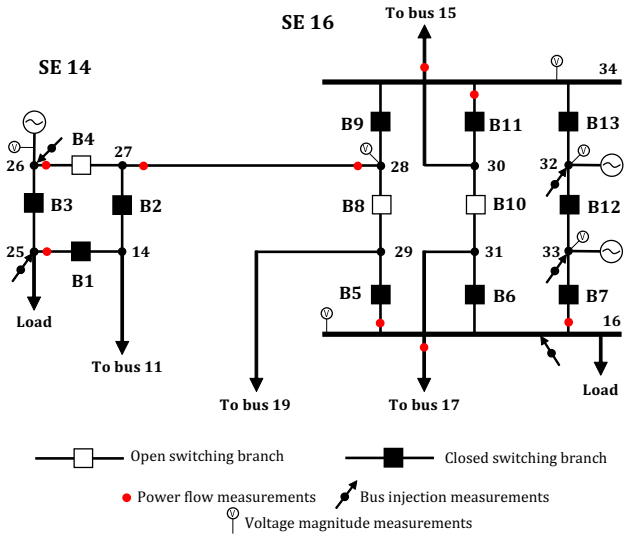

Fig. 2. Details of substations 14 and 16 of IEEE 24-bus test system.

iterations, and also indicates how the pseudo-measurements perceived as erroneous (see Section IV-B) are progressively captured in the set of outliers S. With σ_{min} set as 0.02, the table also shows that the outer iteration loop converges in four iterations, and all power flows through the switching devices with wrong statuses are correctly identified (due to the low σ_{min} value, a sound analog measurement, P_{21}, is also included in set S). The average number of inner loop iterations per outer loop iteration has been 2.75.

TABLE I
EVOLUTION OF OUTER LOOP RESULTS FOR CASE B-1

$iter_{out}$	σ^k	Set S of Outliers	σ^{k+1}
1	10	$\emptyset$	4.130
2	4.130	$\{t_{B9}, u_{B9}\}$	4.053
3	4.053	$\{t_{B9}, u_{B9}, t_{B2}, u_{B2}\}$	0.031
4	0.031	$\{t_{B9}, u_{B9}, t_{B2}, u_{B2}, P_{21}\}$	0.014

The post-processing stage of Section IV-C is finally applied in order to determine the estimated topology. Table II presents the switching branch power flows, along with the ϵ_{flow} threshold values computed for a false alarm probability of 5%. In the last column, 0 (1) indicates an open (closed) switching branch. Values in boldface indicate breakers whose statuses have been revised by the proposed algorithm. It can be seen that only for the truly open circuit breakers the flows are less than the corresponding threshold.

Finally, the computed values for the bus voltage and switching branch flow metrics defined in (18) and (19) are $M_V = 0.07\%$ and $M_S = 0.48\%$, respectively. Since both values easily satisfy the performance standards stated in the end of Section V-A, and also the topology has been correctly estimated, we conclude that the state & topology coestimation has been successfully performed.

2) Simultaneous occurrence of topology error and analog bad data: As in the previous case, the presumed topology is

TABLE II
SWITCHING BRANCH POWER FLOWS AND ESTIMATED TOPOLOGY

Switching branches	Active Power Flow		Reactive Power Flow		Estimated Status
	ϵ_{flow}	Estimated	ϵ_{flow}	Estimated	
B1	0.0293	1.9402	0.0164	0.2522	1
B2	0.0330	4.0571	0.0195	0.2045	**1**
B3	0.0252	0.0016	0.0201	0.1364	1
B4	0.0185	0.0009	0.0161	0.0004	0
B5	0.0219	0.6753	0.0181	0.3293	1
B6	0.0338	3.2202	0.0223	0.3239	1
B7	0.0294	1.5410	0.0186	0.4523	1
B8	0.0287	0.0025	0.0224	0.0007	0
B9	0.0359	4.1390	0.0252	0.3627	**1**
B10	0.0299	0.0002	0.0211	0.0013	0
B11	0.0253	1.0483	0.0181	0.3419	1
B12	0.0349	2.3210	0.0242	0.5786	1
B13	0.0374	3.0907	0.0257	0.7046	1

erroneous due to wrong reported statuses of circuit breakers $B2$ and $B9$; now, however, analog bad data are also simulated, by adding errors with magnitudes equal to 15 standard deviations to three analog measurements, namely: V_{15}, P_{19} and Q_{19}.

TABLE III
EVOLUTION OF OUTER LOOP RESULTS FOR CASE B-2

$iter_{out}$	σ^k	Set S of Outliers	σ^{k+1}
1	10	$\emptyset$	4.155
2	4.155	$\{t_{B9}$,$u_{B9}\}$	4.028
3	4.028	$\{t_{B9}, u_{B9}, t_{B2}, u_{B2}\}$	0.204
4	0.204	$\{t_{B9}, u_{B9}, t_{B2}, u_{B2}, V_{15}, P_{19}\}$	0.073
5	0.073	$\{t_{B9}, u_{B9}, t_{B2}, u_{B2}, V_{15}, P_{19}, Q_{19}\}$	0.043
6	0.043	$\{t_{B9}, u_{B9}, t_{B2}, u_{B2}, V_{15}, P_{19}, Q_{19}, t_{15-21}\}$	0.022
7	0.022	$\{t_{B9}, u_{B9}, t_{B2}, u_{B2}, V_{15}, P_{19}, Q_{19}, t_{15-21}$, $t_{28-27}\}$	0.013

Table III shows the evolution of σ values along the outer loop iterations, and also indicates how measurements identified as erroneous are progressively included in the set of outliers S. For $\sigma_{min} = 0.02$, the table shows that in this case the outer loop converges in seven iterations. All power flows through the switching devices with wrong statuses, as well as analog bad data, are correctly identified, although two sound branch flow measurements are also included in set S. The bus voltage and switching branch flow metrics values for this case are $M_V = 0.11\%$ and $M_S = 0.58\%$, figures which are also compliant with the previously stated performance standards. Since the topology has also been correctly estimated, it is once more concluded that the proposed coestimation has been successful.

A final remark is in order concerning the sound measurements misidentified as outliers in the two case studies performed for the 24-bus network. As previously suggested in Section IV-B, the size of set S (as well as the number of outer iterations) is strongly dependent on the value of parameter σ_{min}, which in both cases has been set as 0.02. From Tables I and III it is possible to conclude that another choice such as, for instance, $\sigma_{min} = 0.05$, would prevent the inclusion of any good measurements in S, in both cases. This stresses the fact that σ_{min} should be seen as a design parameter to be carefully chosen in order to reduce such occurrences as much as possible.

C. Results for the IEEE 30-bus system

For this larger test system, we concentrate on the overall performance appraisal of the proposed coestimation approach in regard to topology estimation only. For that purpose, it is assumed that the bad data pocket submitted to PSSE second stage comprises five substations, whose circuit breaker arrangements are displayed in Figure 3. Altogether, 25 switching branches are explicitly modeled.

Exhaustive simulations have been performed considering all possible cases for the occurrence of: no topology errors; one breaker status error; two simultaneous errors, and three simultaneous errors in the presumed network topology. Due to the combinatorial nature of the problem, it can be easily concluded that the total number of possible cases grows significantly with the number of simultaneous errors. For instance, considering two simultaneous breakers with wrong statuses among the whole population of 25 breakers generates $\binom{25}{2} = 300$ distinct cases.

After simulating all above cases, statistical indices for the outer and inner iterative loops of the algorithm, as well as mean values for the performance metrics (18) and (19), have been determined for each batch of cases corresponding to the above four subcases, each of which with distinct numbers of simulated errors. Those results are presented in Tables IV and V.

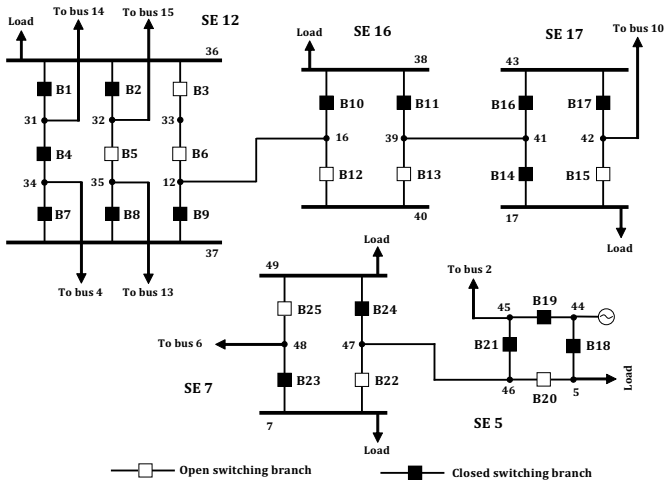

Fig. 3. Details of substations 5, 7, 12, 16 and 17 of IEEE 30-bus test system.

TABLE IV
STATISTICAL INDICES FOR ITERATIVE LOOPS - CASE C

Number of Topology Errors	Number of Cases	$iter_{int}$		$iter_{out}$	
		Mean	Median	Mean	Median
0	1	3.50	3.50	2.00	2.00
1	25	3.13	3.00	3.16	3.00
2	300	2.92	2.50	3.76	4.00
3	2298	2.69	2.33	4.27	4.00

TABLE V
AVERAGE VALUES OF VOLTAGE AND FLOW METRICS - CASE C

Number of Topology Errors	Number of Cases	$M_V(\%)$	$M_S(\%)$
0	1	0.1659	0.1872
1	25	0.1932	0.2586
2	300	0.2125	0.2420
3	2298	0.2082	0.2411

Results in Table IV clearly show that the number of outer loop iterations, $iter_{out}$, tends to grow with the number of simultaneous errors in the presumed topology, as expected. On the other hand, the number of inner iterations per outer loop iteration, $iter_{int}$, exhibits a slight decrease as $iter_{out}$ grows. As for the complex voltage and flow performance metrics, results in Table V indicate that there is no significant degradation of both indices as the number of simultaneous errors increase.

We can thus conclude that for the 2624 cases reported in Table IV, the MCC state & topology coestimation method complies with the adopted standards for successful performance, implying that all errors considered in the reported cases are properly identified and corrected. In only two cases, not included in Tables IV and V, the method have failed to converge, so that the standards for performance success are not fulfilled. Both unsuccessful cases are connected with the simultaneous occurrence of three particularly severe breaker status errors. Therefore, the success rate for three simultaneous errors in breaker statuses is 99.91% $(2298/2300)$, while the same index reaches 100% for the occurrence of both one and two errors. The success rates for all 30-bus system case studies containing topology errors are summarized in Table VI. It is also worth noticing that, in the absence of analog bad data, all converge cases have produced the correct network topology.

TABLE VI
SUCCESS RATES - CASE C

Number of Topology Errors	Number of Cases	Number of Successful Cases	Success Rate
1	25	25	100 %
2	300	300	100 %
3	2230	2298	99.91 %

VI. CONCLUSIONS

A novel, recently proposed power system state estimation approach based on the maximum Correntropy principle and the accessory use of dynamically adjusted Parzen windows is extended in this paper in order to include topology error processing. The above concepts from Information Theory aim at extracting the maximum amount of information from observable information available on a given system. In this paper, topology information as represented at the bus-section level is modeled as pseudo-measurements subject to uncertainty. Such procedure allows that switching branch statuses be treated in a similar manner as analog measurements. Therefore, both types of data can equally benefit from the screening and self-healing properties of maximum correntropy-based state estimators. This enables the resulting estimators to perform both state and topology estimation without the need of costly post-processing stages for bad data detection and identification.

The proposed state & topology coestimation method has been tested by using several case studies derived from the IEEE 24-bus and 30-bus benchmark systems. The results confirm the robustness of the proposed methodology in the presence of both analog bad data and erroneous switching branch statuses that are the main cause of topology errors.

REFERENCES

[1] F. C. Schweppe and J. Wildes, Power System Static-State Estimation, Part I: Exact Model *IEEE Trans. on Power Apparatus and Systems*, vol. 3, no. 4, pp. 120-135, Jan 1970.

[2] A. Monticelli, *State Estimation in Electric Power Systems: A generalised Approach*, Springer, 1 edition, May 1999.

[3] A. Abur and A. G. Exposito, *Power System State Estimation: Theory and Implementation*, CRC Press, 1 edition, March 2004.

[4] E. M. Lourenco, A. S. Costa, K. A. Clements and R. A. Cernev, "A Topology Error Identification Method Directly Based on Collinearity Tests", *IEEE Transactions on Power Systems*, vol. 21, pp. 1920-1929, 2006.

[5] A. G. Exposito and A. de la Villa Jaen, "Reduced substation models for generalized state estimation," in *IEEE Transactions on Power Systems*, vol. 16, no. 4, pp. 839-846, Nov 2001.

[6] N. Vempati, C. Silva, O. Alsac and B. Stott, "Topology Estimation", *IEEE PES - Power Engineering Society General Meeting*, vol. 1, pp. 806-810, June 2005.

[7] N. S. da Silva, A. S. Costa, K. A. Clements and E. Andreoli, "Simultaneous estimation of state variables and network topology for power system real-time modeling", *Electric Power Systems Research*, vol. 133, pp. 338-346, April 2016.

[8] V. Freitas and A. S. Costa, "Integrated State & topology estimation based on a priori topology information", *2015 IEEE Eindhoven PowerTech*, pp. 1-6, Eindhoven, 2015.

[9] W. Liu, P. P. Pokharel and J. C. Principe, "Correntropy: Properties and applications in non-gaussian signal processing", *IEEE Transactions on Signal Processing*, v. 55, n. 11, p. 5286-5298, Nov. 2007.

[10] E. Parzen, "On estimation of a probability density function and mode", *Annals of Matlhematical Statistic*, vol. 33, pp. 1065-1076, Sep. 1962.

[11] J. K. Opara, "Information Theoretic State Estimation in Power Systems", PhD thesis, Faculdade de Engenharia da Universidade do Porto, Dec. 2013

[12] V. Freitas, A. S. Costa and V. Miranda, "Robust State Estimation based on Orthogonal Algorithms and Maximum Correntropy Criterion", accepted for presentation at the 2017 IEEE PowerTech, Manchester, June 2017.

[13] V. Miranda, A. Santos and J. Pereira, "State Estimation Based on Correntropy: A Proof of Concept", *IEEE Transactions on Power Systems*, vol. 24, no. 4, pp. 1888-1889, Nov. 2009.

[14] W. Wu, Y. Guo, B. Zhang, A. Bose and S. Hongbin, Robust state estimation method based on maximum exponential square, *IET Generation, Transmission Distribution*, vol. 5, no. 11, pp. 1165-1172, Nov. 2011.

[15] O. Alsac, N. Vempati, B. Stott and A. Monticelli, "Generalized state estimation," in IEEE Transactions on Power Systems, vol. 13, no. 3, pp. 1069-1075, Aug 1998.

[16] K.A. Clements and A. S. Costa, "Topology error identification using normalized Lagrange multipliers", *IEEE Tans. Power Systems*, vol. 3, pp. 347-353, May 1998.

[17] E. M. Lourenco, A. S. Costa and K. A. Clements, "Bayesian-based hypothesis testing for topology error identification in generalized state estimation", *IEEE Transactions on Power Systems*, vol. 19, no. 2, pp. 1206-1215, May 2004.

[18] A. Monticelli, "Modeling circuit breakers in weighted least squares state estimation", in *IEEE Transactions on Power Systems*, vol. 8, no. 3, pp. 1143-1149, Aug 1993

[19] P. M. Subcommittee, "IEEE Reliability Test System," in *IEEE Transactions on Power Apparatus and Systems*, vol. PAS-98, no. 6, pp. 2047-2054, Nov. 1979

[20] R. Billinton, P. K. Vohra and S. Kumar, "Effect of Station Originated Outages in a Composite System Adequacy Evaluation of the IEEE Reliability Test System," in *IEEE Power Engineering Review*, vol. PER-5, no. 10, pp. 25-26, Oct. 1985.

[21] A. Abur, Hongrae Kim and M. K. Celik, "Identifying the unknown circuit breaker statuses in power networks," in *IEEE Transactions on Power Systems*, vol. 10, no. 4, pp. 2029-2037, Nov. 1995.

[22] KEMA. Metrics for Determining the Impact of Phasor Measurements on Power System State Estimation. *Eastern Interconnection Phasor Project*, March 2006.